Published in final edited form as:
Semin Immunopathol. 2010 September ; 32(3): 305–317. doi:10.1007/s00281-010-0217-9.

Intravital imaging of anti-tumor immune response and the tumor microenvironment

Tomasz Zal and
Department of Immunology, University of Texas MD Anderson Cancer Center, Unit 902, 1515 Holcombe Blvd., Houston, TX 77030, USA

Grzegorz Chodaczek
Department of Immunology, University of Texas MD Anderson Cancer Center, Unit 902, 1515 Holcombe Blvd., Houston, TX 77030, USA

Tomasz Zal: tzal@mdanderson.org

Abstract

Tumor growth, invasiveness, and metastasis are dynamic processes involving cancer interactions with the extracellular matrix, the vasculature, and various types of non-cancerous host cells that form the tumor stroma. An often-present stromal component is the immune cells, such as tumor-associated myeloid and lymphocytic infiltrates, yet endogenous anti-tumor immune responses are typically ineffective in tumor rejection and may even contribute to the progression of some cancers. How exactly cancer cells interact with the stroma and invade healthy tissues while avoiding anti-tumor immune responses, and which interactions should be targeted for anti-tumor therapy, can now be studied by minimally invasive observation using multi-photon and other low impact confocal microscopy techniques and fluorescent animal tumor models. Intravital video microscopy has already been instrumental in defining the roles and modes of cellular motility in the angiogenic process and during tissue invasion at the tumor margin. In the hands of cancer immunologists, intravital video microscopy is beginning to unravel the complexity of effector and suppressory lymphocytic interactions in tumors and in the draining lymphoid organs. As the intravital microscopy approach is beginning to move beyond fundamental description and into analyzing the molecular underpinnings of cell's dynamics, future technical advances will undoubtedly provide yet deeper insight while stitching together a systems dynamics view of cancer–host interactions that will keep on inspiring cancer researchers and therapists.

Keywords

Multiphoton microscopy; Intravital imaging; Tumor microenvironment; TIL; Regulatory FoxP3$^+$ T cells; Tumor-associated macrophages; Immunotherapy

Introduction

Besides uncontrolled proliferation, tumor pathogenicity is attributable to malignant cell migration, which contributes to tumor invasiveness and metastatic potential (Fig. 1). When migrating between other cells and through the extracellular matrix (ECM), cancer cells can cause tissue damage and remodeling. Some migratory cancer cells can traverse epithelial

Correspondence to: Tomasz Zal, tzal@mdanderson.org.

This article is published as part of the Special Issue on Immunoimaging of Immune System Function.

barriers and enter blood circulation to disseminate in new locations. Cancer cell motility is thus harmful and constitutes an important target for therapeutic intervention. On the other hand, however, cellular motility is required for the surveillance and effector functions of the immune system, which has the capacity to recognize cancers and mount therapeutically valuable anti-tumor immune responses. To be effective, tumor-specific cytotoxic T lymphocytes (CTL) must first interact with antigen-presenting dendritic cells (DC) that migrate from the tumor to the draining lymph nodes to cross-present tumor antigens. CTL motility is then critical to home to and infiltrate the tumor mass and engage in direct killing interactions with cancer cells. While it is possible and, indeed, informative to study the migratory characteristics of malignant or immune cells under in vitro conditions, critical information is inevitably lost about the spatiotemporal regulation that takes place in the 3D environment of living tissues. Particularly difficult to reproduce is the impact of the vascular blood flow and the lymphatics function on such events as metastasis or immune cell recruitment. It is likewise difficult to recreate ECM, in which cells move through fibrillar protein networks and respond to chemotactic gradients. It is thus with a great enthusiasm that cancer biologists and immunologists welcomed the development of multiphoton microscopy (MPM) and novel fluorescent cell labeling methods that allowed high-resolution visualization of cellular behaviors in intact living tissues and intravital preparations.

Over the recent decade, MPM was applied to address a variety of questions in tumor biology and immunology, each field exploring the behavioral characteristics of the cells that they study. For the most part, cancer biologists and immunologists who embarked on intravital imaging projects were working in separation. Incidentally, significant breakthroughs were made by others that led to defining the molecules, such as CTLA4 [1], and immune cell types, such as the $CD4^+$ $FoxP3^+$ regulatory T cells (T-reg) [2–4], that began explaining why anti-tumor immune responses are so ineffectual. Since then, cancer immunology is undergoing revival, and new potentially powerful anti-tumor immune therapies directed against the immune-suppressory pathways are being tested in the clinic. It is still unclear, however, how exactly the immune system interacts with cancer at steady state and during therapy, enticing both cancer biologists and immunologists to join forces applying MPM and other intravital imaging techniques to reveal such interactions in intact tumors.

Advantages of MPM and other low impact confocal microscopy for cancer and immunology research

MPM is a variation of conventional laser scanning confocal microscopy (LSCM) that excels in the depth of imaging in light scattering specimens, such as tissues, and by greatly limiting laser phototoxic damage to living cells. As such, MPM has become the method of choice for the investigation of single cell dynamics in living tissue specimens and in vivo [5]. The key advantages of MPM come from using ultra short-pulsed near-infrared lasers instead of continuous visible and ultraviolet lasers that are typical for LSCM. Unlike the continuous, hence relatively low intensity illumination, femtosecond pulsed near-infrared lasers distribute the same average power into highly intense light packets. As the light intensity is further focused by the objective lens, fluorophores can become excited by almost simultaneously absorbing two (or more) low energy near-infrared photons, thus generating fluorescence with an intrinsic optical sectioning ability, i.e., without the need for a confocal pinhole. Highly sensitive wide field non-descanned detection is therefore applicable that can efficiently gather photons emitted and scattered deep in tissues. The phototoxic effects of multiphoton excitation are likewise confined to the focal plane only, while the linearly scaling adverse effects, such as infrared heating, are largely avoided at low average laser powers [6].

In addition to fluorescence-based contrast, MPM allows label-less or intrinsic contrast imaging. The primary sources of intrinsic contrast in MPM are the fibrillar collagen and elastin, which

are the primary ECM constituents, as well as certain cellular metabolites. The underlying mechanisms of signal generation are twofold. Collagen fibers and other highly repetitive chiral structures interact with femto-second light pulses causing nonlinear light scattering and interference, termed second harmonic generation (SHG), which produces visible light of exactly half the wavelength of the illumination [7,8]. While SHG is the most intense in the forward direction, it can be acquired in the back-scattered direction using high numerical aperture objectives, therefore being applicable to thick tissues and intravital preparations. Elastin, on the other hand, and certain cellular metabolites, such as nicotinamide adenine dinucleotide (NAD, NADH) and flavin adenine dinucleotide (FAD), emit intrinsic two-photon excited autofluorescence, each at its characteristic, rather broad range of wavelengths [9–11]. The structure of the ECM can thus be revealed by simultaneous imaging of collagen SHG and elastin autofluorescence. Intracellular redox states can be assessed by imaging the NAD/FAD ratios, which is of interest to visualize tumor hypoxia.

Leaping improvements have also been made in the conventional, single photon microscopy domain, resulting in new low impact confocal techniques that are applicable to intravital imaging. Rapid resonant scanning LSCM and spinning disk confocal microscopy are particularly notable in that regard, offering low phototoxicity at high temporal and spatial resolutions, although not as deep axial penetration as MPM. The improvements can be traced to much shorter laser beam dwell times allowing the excited triplet states to dissipate prior to photochemical fluorophore inactivation, as well as, in spinning disk confocal microscopes, more efficient, camera-based detection. Resonant scanning is also applicable to MPM, further improving temporal resolution and decreasing phototoxicity [12] (and our unpublished data). While other, lower resolution intra-vital imaging techniques are increasingly used for tumor imaging, for example, nuclear radiotracer imaging and whole body fluorescence imaging, only MPM and the low impact confocal microscopy techniques provide the necessary combination of subcellular spatiotemporal resolution, biocompatibility, and multiplex detection that is necessary to reveal individual cell interactions.

Fluorescent labeling strategies to reveal cell populations and tumor microenvironment

Visualizing individual cell behavior in vivo generally requires appropriate fluorescent labeling of pre-determined cell populations. In general, two labeling strategies are applicable: by ex vivo labeling of purified cell populations with fluorescent dyes or genetically-encoded fluorescent proteins, followed by adoptive transfer to syngeneic mice, and by using fluorescent reporter transgenic mice. Dye dilution in proliferating cells limits the usefulness of chemical labeling for long experiments (while allowing the number of cell divisions to be measured), which can be avoided by retroviral expression of fluorescent proteins. By using lineage-specific fluorescent protein reporter transgenic mice as tumor recipients, truly endogenous host cells can be followed indefinitely in their entirety, allowing a quantitative outlook over the cell's representation. Deregulation of tumor vasculature and vascular leakage, which are hallmarks of the tumor microenvironment, can be visualized by intravenous injection of high molecular weight fluorescent dextrans or quantum dots. Alternatively, the vasculature can be visualized in vivo using reporter mice expressing green fluorescent protein (GFP) under the epithelial Tie-2 kinase promoter [13]. Angiogenesis can be monitored using the nexin promoter-GFP mouse strain, which reveals the nascent blood vessels [14].

Intravital tumor preparations for time-lapse microscopy

Skilled surgery and stable positioning are critical for successful intravital time-lapse fluorescence microscopy, as even slight movements due to bodily functions, such as breathing or heartbeat, can render the data unusable. Stable tumor positioning for vital imaging studies

has been possible before the advent of MPM using a skin-fold chamber/window device [15, 16]. Cancer cells are placed underneath a glass window in the skin stretched on the back of the animal. If the growth is sufficiently shallow, the skin flap model is optically compatible with various imaging modalities, including camera-based (wide field and spinning disk confocal), LSCM, as well as MPM.

The skin-fold window was applied to a human HT-1080 fibrosarcoma model implanted in immune-compromised recipient mice to study the growth rates, tumor-induced angiogenesis, and tissue invasion [17]. By expressing the DsRed2 red fluorescing protein in the cytoplasm and histone 2B linked to enhanced GFP (H2B-EGFP) in the nucleus, the tumor volume (based on the DsRed2 signal) and the frequency of mitosis (based on the nucleus shape) could be measured, demonstrating the high spatial resolution attainable with this technique. Longitudal imaging of the same area showed that tumor volume increased faster after the onset of angiogenesis (days 3–4 after implantation). The frequency of mitosis (2–5%) and apoptosis (<1%) could be estimated based on the ratios of the nucleus to cytoplasm areas and nuclear morphology. The skin flap window preparation is thus invaluable for the longitudal studies of angiogenesis in small tumors [18].

The drawbacks of the skin flap window model include poor thermoregulation, adverse tissue reactions, and limited tumor size. Moreover, the skin flap model does not fully recapitulate the intricacies of non-skin tumors—an important dilemma for cancer researchers and tumor immunologists interested in orthotropic tumor models and tissue-dependent immune responses. Modified tumor window preparations are now possible for breast cancer [19] and bone or bone marrow cancers, the latter using a cranial bone window preparation [20]. Our own studies are focused on the lungs, an organ that is a physiological target of tumorigenesis and metastasis but a challenging one to image due to the breathing action. The strategy that we applied is based on a suction device similar to that described for rat lung positioning [21]. When miniaturized and equipped with electro-thermal control systems, the lung holder device enables stable intravital imaging of tumor metastases in surgically exposed, breathing lungs (Fig. 2).

Intrinsic contrast MPM imaging of the ECM and cell metabolism

Increased deposition of collagen, or desmoplasia, is a characteristic of many tumors [22]. By using SHG and tissue autofluorescence-based MPM, ECM was analyzed in esophageal cancer at different clinical stages, showing that desmoplastic collagen fibers lost their typical fine structure and their area became reduced [9]. In contrary, the amount of elastin in neoplastic stroma was increased, with elastin fibers becoming shorter and more fragmented, compared to healthy tissues. In a breast cancer model, tumor-associated collagen signatures were identified that could be used as characteristic markers of tumor expansion [23]. In addition, cancer-affected tissues changed their intrinsic femtosecond pulse-excited autofluorescence and morphological characteristics. Using intrinsic contrast MPM, at least five autofluorescence-detectable features could be identified in 7,12-dimethylbenz(a)anthracene-inducible hamster cheek squamous carcinomas that were diagnostically distinct when compared to normal epithelium: the nuclear density ratio, the keratin layer and epithelial thickness, and the fluorescence intensity in the keratin and epithelial layers [24].

Rapid tumor growth and poor vascularization often result in tumor hypoxia, which causes cells to switch from the oxidative phosphorylation to glycolysis [25–28]. The altered cellular respiration is detectable by MPM imaging of the intracellular ratios of the reduced form of NAD (NADH) and the oxidized form of FAD. In addition to altering the relative intensities of NADH and FAD, which can be assessed ratiometrically, intracellular redox states also affect fluorescence lifetimes, whose measurements are intrinsically compatible with pulsed excitation [10,11]. It was possible that way to differentiate precancerous or cancerous cells from the

surrounding normal tissue, as well as the invading metastatic cells from noninvasive cells, all without additional fluorescent labeling [29–33]. Since no fluorescence labeling is required, SHG and intrinsic autofluorescence MPM hold promise for noninvasive imaging of human tissue biopsies and in vivo subjects [34]. By combining SHG with cell tracking, cellular motility can be studied in relation to the ECM structure [35–38].

Tumor cell migration and tissue invasion

Tumor pathogenesis is primarily attributed to tumor invasiveness, which is largely determined by the migratory behavior of cancer cells towards and into the surrounding tissue (Fig. 1). Intravital MPM was instrumental in revealing two distinct modes of cancer cell motility, as distinguished by morphological changes during cell movement [39,40]. The migration of cells with spindle-like shape, termed mesenchymal or fibroblastic migration, proceeds via pseudopod protrusion at the leading edge, followed by focal attachment to the ECM, and detachment of the trailing edge. To pass through the fibrous ECM networks without inflicting excessive distortion to the rigid nucleus, cancer cells created openings between the fibers to then squeeze through the openings. Indeed, the mesenchymal migration was associated with ECM degradation and formation of tube-like tracks lined with ECM degradation products. The dynamics of ECM degradation and cell translation depended on a matrix metalloproteinase (MMP) activity at the focal attachment points as well as integrin-driven adhesion. Interestingly, upon inhibiting extracellular proteases, tumor cells underwent a mesenchymal-amoeboid transition. In particular, they acquired a more spherical morphology, became highly deformable, and instead of digesting their way through the ECM, moved in a propulsive, amoeboid manner by cytoplasmic streaming and squeezing [41]. The amoeboid movement was associated with short-lived and weak interactions with the substrate, allowing the cells to reach higher velocities. The process of mesenchymal-amoeboid motility transition could be involved in increasing tumor invasiveness and, if it enables cancer cells crossing into the blood circulation, it could increase metastasis.

Collective cell movement refers to coordinated translational motility of cell sheets, aggregates, or clusters migrating as a functional unit [42–44]. Multiphoton imaging of a sarcoma tumor margin revealed that cancer cells could proceed into the surrounding tissue in a collective manner by assembling and migrating together in highly asymmetrical multicellular strands [17]. The cells at the leading edge were highly motile, guiding the cells that followed, whereas the cells in the inner and rear regions of the collective movement unit were pulled passively. The pack's movement through the collagen network was facilitated by membrane-bound MMPs on the anterior cells. The MMP activity cleaved collagen fibers in such a way that the fibers become aligned parallel to cell body to form tracks of least mechanical resistance, thus facilitating the passage of the cells that followed [45]. The consecutively passing cells further amplified the process, such that large macrotracks formed that guided the collective invasion. In addition to MMPs, the joint movement also depended on the activity of β1 integrin. Upon blocking both β1 integrins and MMPs, the collective cell motility pattern was abolished, transitioning to more random singular motility; a similar phenomenon was also triggered by TGFβ signaling [43,45,46]. Interestingly, the ECM-derived peptides that were produced by tumor-mediated proteolysis further stimulated cancer cell motility, suggesting a chemokinetic positive feedback loop that could enhance cancer cell migration and tissue invasion [40,47].

The acquisition of migratory behavior by cancer cells is suspected to contribute to metastasis, a poorly understood process of remote tissue colonization requiring, at an initial stage, cancer cell intravasation into the bloodstream or the lymphatics. Interestingly, intravital tracking of quantum dot-labeled tumor cells in mice showed that, in addition to the hematogenous and lymphatic routes, cancer cells can use primo-vessels—semitransparent fluid-conducting multilumen channels—to disseminate and form metastases in the peritoneum [48]. Using MPM, the

migratory capacity of non-metastatic and metastatic cells was compared in primary mammary carcinoma tumors [49]. The cells of the metastatic line MTLn3 interacted more often with collagen fibers than the non-metastatic MTC cells, despite higher collagen content in the non-metastatic tumors. Although their migration rates were similar (3.4 μm/min), the metastasis-prone MTLn3 cells tended to move in a more linear fashion along collagen fibers, stopping whenever fibers were missing. The metastatic capacity also correlated with the ability of tumor cells to reorganize the collagen networks [23,50]. In the vicinity of blood vessels, the metastasis-prone MTLn3 cells polarized and migrated toward the vessels, indicating sensitivity to a guiding gradient—a behavior that contrasted with mostly random motility of non-metastatic MTC cells. Epidermal growth factor receptor (EGFR) could be involved in the cell guidance since metastatic tumors had high levels of EGFR and responded to EGF gradients [49], which originated from tumor stroma and vasculature [47]. Indeed, over-expression of EGFR in MTC cells increased their chemotactic responses to EGFR ligand in correlation with the metastatic potential [51]. Only few MTC cells were observed entering the blood vessels, and those that did underwent fragmentation due to the hydrodynamic shearing of pseudo-pods that penetrated into the blood stream, resulting in the cell's death by apoptosis. The intravasating MTLn3 cells, in contrast, remained intact, their mechanical stability being greater due to increased cytokeratin content. The results of the experiments with the implanted MTLn3 and MTC cell lines, which were further corroborated in spontaneous tumor models [52], support the notion that the acquisition of metastatic potential by cancerous cells can be in part attributed to a coordinated deregulation of multiple pathways involved in directional cell motility, including chemotaxis, ECM-mediated guidance, and cellular polarization.

Intravital imaging showed a spatial heterogeneity in the ability of tumor cells to migrate within tumors [53]. Using a chronic cranial window, the motility of red fluorescent protein (RFP)-expressing glioma was recorded in vivo in relation to blood vessels, which were visualized by intravenous injection of high molecular weight fluorescein isothiocyanate-dextran. Tracked over 48 h, the cells migrated predominantly away from the tumor center (84% of cells), stretching out along the abluminal site of the endothelial cells of brain microvessels (91% of cells). The speed of perivascularly moving cells, while relatively slow (0.024 μm/min), was 3.6-fold higher than the cells positioned away from capillaries. The perivascular cancer cell motility coincided with vessel remodeling, capillary dilation, vessel splitting, and glomeruloid bodies (loops) formation.

The mechanisms of tumor invasiveness were further corroborated in a breast cancer window model [54]. Orthotopically implanted mammary tumor MTLn3 cells expressed the photoswitchable protein Dendra2, whose fluorescence can be changed from green to red by intense UV illumination, thus allowing individual cells to be marked. In the region that lacked discernable blood vessels, UV-photomarked cancer cells stayed close together, whereas in the vascularized regions, photomarked cancer cells spread out over a larger area, demonstrating a higher migratory potential. A faster drop in the number of photo-marked cells in the vascularized region suggested ongoing intravasation. It is thus likely that tumor vascularization can increase its metastatic potential by affecting cancer cell migration.

To study the mechanisms of cancer cell extravasation, leukemic cells were injected intravenously and followed in the bone marrow. Circulating metastatic cancer cells extravasated preferentially in distinct "hot spot" sites that were demarcated by increased concentration of the vascular cell adhesion molecule E-selectin and the SDF-1 chemokine [55]. Interestingly, not only leukemic cells but also hematopoietic stem/progenitor cells and lymphocytes used the same hot spots to arrive in bone marrow. SDF-1 binding to its receptor CXCR4 was critical, since CXCR4 blockade and/or downregulation inhibited cancer engraftment.

Angiogenesis and metastasis establishment

Once blood-carried metastatic cancer cells lodge in a target tissue to form micrometastases, their survival depends on physical proximity to a blood vessel for nutrient access. Beyond a submillimeter size, further growth requires successful neovascularization. The early stages in metastasis establishment were studied by comparing melanoma and lung carcinoma interactions with brain capillaries in a chronic cranial window preparation [56]. The initial stages were similar: arriving cancer cells became arrested at microvascular branches due to size restriction, followed by extravasation over the following 3 days. After that, the cells stayed close to the vessel wall and maintained a direct contact with abluminal endothelial cells—an interaction that was essential for their survival [56]. From then on, different strategies were employed by the melanoma and carcinoma micrometastases to ensure sufficient blood supply. Melanoma micrometastases could grow as big as ~380 μm without triggering angiogenesis and vascularization, but carcinoma micrometastases triggered early vascularization, after reaching a diameter of~150 μm, which could be related to the production of vascular epidermal growth factor (VEGF) by the carcinoma but not melanoma cells. But how could the melanoma grow up to ~380 μm without forming new vessels? Interestingly, by migrating along micro-vessels, melanoma cells distorted them into small loops, thus increasing the micrometastasis-to-vessel contact area without new vessel formation. Two critical, vasculature-dependent phases of metastasis development were thus identified by dynamic imaging: the angiogenesis-independent growth of perivascular micrometastases, and the VEGF and angiogenesis-dependent transition from micro- to macro-metastases [56].

Antiangiogenic therapeutics is pursued to slow down tumor growth by depriving it of blood supply. Sunitinib is a multi-targeted tyrosine kinase inhibitor that exhibits multiple, including antiangiogenic, effects by interfering with the VEGF receptor and other Stat3-dependent growth factor receptor signaling, but the exact mechanism of its efficacy is not clear [57]. Using intravital microscopy in a renal carcinoma model and intravital annexin V staining to reveal apoptosis, the effects of sunitinib were followed in vivo soon after treatment. Interestingly, tumor apoptosis was apparent as early as 1 day after administering the agent and before the collapse of tumor vasculature, thus revealing a previously unappreciated, non-antiangiogenic activity of sunitinib and demonstrating the potential of intravital microscopy to study pharmacological function.

Visualizing the role of tumor stroma in cancer cell dynamics: TAM and TAF

Among the most reliably found stromal components in most tumors are tumor-associated fibroblasts (TAF) and macrophages (TAM), both of which were implicated in promoting tumor growth and progression. In agreement with histological observations, intravital microscopy showed that TAM tended to concentrate at the tumor margin [58–60], as well as associating with blood vessels inside tumors as single cells or small clusters. Time-lapse recordings showed that TAMs, which can be labeled in vivo with fluorescent dextrans and other cell-ingestible contrast agents, were motile, moving with the median speed of 2.9 μm/min, which was faster than tumor cells (1.8 μm/min), but slower than activated tumor antigen-specific CTL (4.2 μm/min) [60]. Both TAMs and tumor cells released chemotactic factors (EGF and colony-stimulating factor 1, respectively) that acted to regulate their motility in paracrine and autocrine manner [59,61,62]. Interestingly, TAMs engaged in close interactions with tumor cells, guiding them outwards and into the surrounding tissue. Perivascular TAM coincided with intravasating tumor cells, suggesting that TAM could assist tumor cells in migrating through the vascular endothelium [59,61,62]. Fibroblast-like cells can be induced by tumor cells to express VEGF, which is normally associated with wound healing [63]. Intact tissue imagery showed that VEGF-active fibroblasts formed a dense, up to 50-μm thick layer around tumors and up to 200-μm thick layers around angiogenic vessels [64]. TAFs were also implicated in relaxin-

dependent collagen fiber remodeling [65], which was dependent on β1 integrin and MMPs. These and other non-imaging studies reinforced the notion of TAM as critical modulators of tumor growth and invasiveness. Whether TAFs modulate tumor cell migration remains unclear.

Intravital imaging of tumor-associated immune activity

Tumor growth can stimulate and modulate the immune system, which in return can exert potent yet opposing influences over tumor progression. Most tumors are more or less antigenic owing to the mutations and gene deregulation, giving rise to tumor antigens and stress molecules, which can be recognized by $\alpha\beta$ and $\gamma\delta$ T cells, NK cells, and other effector lymphocytes. In a process known as anti-tumor immune surveillance, precancerous and cancerous cells can thus be deleted (reviewed by Dunn et al. [66]). Likewise, the growth of advancing cancers can be counteracted by tumor-infiltrating NK cells and tumor-specific CTLs, as indicated by a reverse correlation between the content of such lymphocytes and the rate of tumor progression in patients and experimental animals. Despite demonstrable anti-tumor cytotoxicity in vitro, however, tumor-infiltrating CTLs are typically ineffectual in the killing of cancerous cells in vivo—an effect that has defined the immune-suppressory properties of the tumor microenvironment. Several mediators of intratumoral immune suppression have been documented, including tumor-associated regulatory T-reg, myeloid-derived suppressor cells (MDSC), and TAM.

What is the role of TCR specificity in T cell homing and migration in tumors?

Some of the most pressing questions in tumor immunology that are being addressed by intravital microscopy concern the mechanism and specificity of T cell recruitment and tumor killing, as well as the role of T-reg. In general, the relative roles of T cell receptor (TCR) specificity versus other non-antigen-specific interactions were studied by visualizing the behavior of fluorescently labeled, adoptively transferred T cells in tumor-bearing mice. Upon adoptive transfer of polyclonal tumor-immune CTL or naive T cells into mice implanted with colon carcinoma, their relative retention in the tumor vasculature was followed in real time [67,68]. As expected, tumor-immune T cells extravasated preferentially while naïve T cells passed by, in agreement with poor retention of naïve T cells in peripheral tissues [68]. In a subsequent study, Ali et al. compared two effector T cell populations, one raised against a tumor and the other against a control antigen [67]. The comparative analysis of the frequency of T cell flow and stoppage in tumor vasculature performed in that study indicated that the tumor-specific, but not the irrelevant peptide-specific, CTLs adhered to the tumor endothelium and extravasated in much higher numbers. In other studies, however, non-tumor-specific CTLs initially accumulated in tumors in only slightly lower numbers compared to tumor-specific CTLs, suggesting that the state of T cell activation and adhesive interactions, but not TCR specificity, were critical for T cell extravasation into tumors [69,70]. In the subcutaneous EL4 thymoma model [69], ovalbumin (OVA)-expressing tumors were confronted by adoptively transferred OVA-specific OT-1 TCR-transgenic CTLs or non-tumor-specific CTLs. Again, the co-transferred tumor-specific and non-tumor-specific CTLs homed into the same tumor in similar numbers and migrated with the average speed limited to 6 μm/min. Later on, however, the tumor-specific T cells but not the control T cells increased their motility over time, which was attributed to TCR-mediated antigen recognition.

In another intravital imaging study, the role of T cell specificity in tumor targeting was dissected in a complementary way by comparing the same OT-1 T cell recruitment to two tumors differing with respect to the expression of the OVA neoantigen [70]. The OVA neoantigen-expressing EG7 or the parental EL4 thymoma cells were implanted subcutaneously followed by adoptive transfer of naïve $CD8^+$ OVA-specific OT-1 T cells, which resulted in the rejection of the OVA-expressing tumor. At the earliest time points, comparable OT-1 T cell numbers

were found in both EG7 and EL4 tumors, which again was in agreement with a TCR-independent mechanism of CTL homing, but in contradiction with the results by Ali et al. Later on, OT-1 T cell density was higher in OVA-expressing tumors, indicating that TCR activation regulated long-term retention and/or cell expansion. The contradiction between the results of Ali et al. [67], who detected tumor-specific T cell extravasation, and those by Mrass et al. [69] and Boissonnas et al. [70], who showed that the extravasation step was not antigen-specific (but was followed by antigen-specific T cell retention and expansion), is not readily explainable but could be rooted in different experimental systems. Polyclonal T cells and a kinetic cell flow analysis of a relatively small number of T cells were used by Ali et al. in contrast to defined TCR T cells and more comprehensive in situ evaluations in the other studies.

In the study by Boissonnas et al., intra-tumor T cell migration was further analyzed in more detail at the early rejection phase, which was defined at the cessation of tumor growth 3–4 days after the transfer, and at a late phase, on days 5–6 when tumors started to shrink [70]. During the early phase, OT-1 CTL motility decreased within antigen-expressing EG7 tumors (mean velocity, 4 μm/min) compared to EL4 tumors (10 μm/min), the cells moving closely to tumor cells and often stopping, indicative of antigen-dependent contact stabilization. In the late phase, when EG7 tumor underwent apoptosis, OT-1 CTLs resumed their migration and behaved similarly as in an EL4 tumor, indicating that the transient slowdown and prolonged interactions coincided with the induction of tumor apoptosis. CTLs often migrated along blood vessels, the cells in close contact with blood vessel becoming more elongated than those further away. In the early phase, most CTLs were located preferentially at the periphery of the tumor (up to 200 μm), although there was no significant difference in the blood vessel density. Later on, during the late rejection phase, the CTL gradient disappeared, and the density of CTL was equal at the periphery and tumor center. In EL4 tumors, CTLs accumulated only at the tumor boundary. A likely trigger for the successful influx of tumor-specific CTLs into the tumor center is a positive inflammatory feedback between tumor killing and increased blood vessel permeability.

TCR specificity and tumor killing

Those early studies did not address the issue how in fact tumors were rejected by CTLs. A direct, CTL-mediated mechanism was one possibility, which would involve the formation of stable contacts between CTL and tumor cells to deliver cytotoxic, perforin, and granzyme-containing granules. That scenario was consistent with the observed prolonged interactions of CTLs with tumor cells. An alternative, indirect mechanism was also possible, whereby the killing was performed by other immune system cells, for example, macrophages or granulocytes activated by CTL-released IFNγ. An imaging study demonstrated elegantly that a direct CTL mechanism was involved in tumor clearance [71]. The experimental strategy was to visualize the behavior of OVA-specific OT-1 CTL in chimeric tumors that were composed of OVA-expressing EG7 cells and OVA-negative EL4 cells (distinguished by yellow or cyan fluorescent protein expression (YFP or CFP), respectively). If both cells were killed equally, such a result would support the indirect mechanism, possibly due to bystander cytotoxic effects of NK cells, macrophages, or granulocytes, for example. Nevertheless, upon adoptive transfer of OT-1 CTL into such mixed tumor-bearing mice, only OVA-expressing EG7 cells were destroyed, and EL4 tumor cells were left intact, demonstrating that antigen recognition of a tumor antigen by CTL on cancer cells is required for selective tumor rejection. When tumor apoptosis was visualized at a single cell level using a caspase 3-sensitive Förster resonance energy transfer (FRET) biosensor, the recordings showed that cancer cell apoptosis was most likely in those tumor cells that interacted with at least one CTL, lending further support to the direct, CTL-mediated mechanism of tumor killing [71]. The possibility of a synergistic involvement of bystander innate effectors could not be ruled out in that system, however.

The molecules that regulate tumor-infiltrating lymphocyte (TIL) migration could be targeted to enhance anti-tumor immunotherapies. Intravital imaging was used to show a role of CD44, a cell surface protein whose intracellular domain can recruit ezrin, radixin, and moesin proteins to the plasma membrane [72]. In contrast to the controls, CD44-deficient TILs migrated at a lower velocity regardless of the presence of the cognate TCR ligand-expressing tumor, and they could not sustain a polarized shape, evident in diminished uropod formation. Even though CD44-deficient TILs interacted with tumor cells for as long as wild-type TILs, the rate of tumor rejection and survival of animals were diminished. CD44-deficient CTLs could not quickly regain their motility after engaging a target cell, indicating that CD44 acted to determine the efficiency of tumor surveillance.

Visualizing lymphocyte interactions during T-reg immune suppression

To study the immune suppressive role of T-reg in modulating anti-tumor CTL activity, Mempel et al. used MPM to visualize cell–cell interactions between adoptively transferred CTLs and surrogate targets (tumor antigen-presenting B cells) in tumor-draining lymph nodes in the absence or presence of tumor antigen-specific T-regs [73]. In the absence of T-regs, CTL killed the sentinel B cell targets (and rejected the primary tumor), which involved CTL attaching to a target cell for 9 to 25 min, prior to cell lysis and CTL detachment. When CTLs were co-transferred with T-regs, both cell populations expanded, indicating antigen recognition, but tumors were not rejected. However, the number of CTL-B cell target conjugates was not changed, and the CTL-target cell interactions were, in fact, prolonged, arguing against a role of T-reg in regulating CTL motility or conjugate formation with target cells. Instead, the suppressory effect was associated with decreased CTL degranulation. Direct interactions between CTLs and T-regs in tumor-draining lymph nodes were rare, indicating that soluble mediators, such as TGFβ, could be involved. One can also envision that, in addition to secreting soluble factors, T-reg effects may be mediated by intermediary interactions with local antigen-presenting cells, such as TAM and DC. How T-regs control anti-tumor immune response in the tumor microenvironment, as opposed to the draining lymph nodes, awaits further investigation.

To determine whether T-reg influence tumor antigen presentation and CTL priming, Boissonnas et al. used intravital microscopy and other approaches to characterize the status of tumor antigen-presenting DCs in tumor-draining lymph nodes [74]. In the presence of T-reg, the number of DCs presenting high tumor antigen densities was decreased, which reduced CTL priming and anti-tumor response. Unexpectedly, tumor antigen-bearing DCs were killed by T-regs in vitro and in vivo in a manner depending on perforin expression in T-reg, thus suggesting that T-reg directly killed DCs. Further, yet still indirect support to this notion was provided by intravital recordings that showed that DC killing correlated with the frequency of DC-T-reg contacts [74]. Interestingly, adoptive transfer of perforin-sufficient non-T-reg T cells into perforin-negative hosts had a seemingly opposite effect, i.e., decreasing DC death, and the effect of perforin-negative T-reg supplementation was not tested. Therefore, whether a direct cytotoxicity of T-reg was indeed operational against tumor antigen-presenting DCs in vivo represents a challenge for future investigations. In addition to raising DC numbers in tumor-draining lymph nodes, T-reg inactivation or depletion affected the dynamics of CTL-DC interactions. In contrast to prior studies showing that co-transferring T-reg with CTL prolonged the duration of CTL-target interactions [73], in this study, an opposite maneuver, i. e., T-reg inactivation or depletion, also increased the duration of CTL-DC interactions, which was unexpected [74]. Since the kind of target cells (B cell tumor cells versus DC) was a main difference between these studies, it is tempting to speculate that T-regs may have different effects upon CTL interactions with tumor targets versus DCs.

Future outlook

While remarkable progress has been made in understanding the spatiotemporal regulation of cell interactions in tumors, even more remains to be uncovered. Several studies revealed how cancer cells move within tumors, invade the surrounding tissues, and metastasize. Further investigation of the effects of pharmacological modulators on the tumor versus stromal cell behavior would go a long way towards providing a mechanistic insight into those processes. Tumor migration-related ECM remodeling and vascular changes could have pronounced influences over the recruitment and behavior of TILs, thus linking tumor–tissue interactions with anti-tumor immune responses. How would T-reg recruitment and suppressory function be affected? Many cancer patients' demise is not due to the primary tumor, but rather due to metastasis development. Studies so far clearly indicate that the frequency of circulating tumor cells far exceeds the rate of metastasis emergence, suggesting tissue defense mechanisms that limit metastasis engraftment. What is the mechanism of the innate and adaptive immune subsystem's involvement in this process requires further investigation.

Future advances in intravital imaging technology

While allowing increased depth of imaging compared to LSCM, MPM does not allow truly deep visualization, which limits the capacity of this imaging modality to visualize the events that take place in the core of large tumors. An increase in the imaging depth is likely by incorporating long wave infrared lasers and optical parametric oscillators, which extend the spectral range of femtosecond lasers beyond 1,100 nm [75,76]. As one reason for image degradation in MPM is defocusing due to tissue curvature and refractive index variations, significant improvements will be realized by applying fast adoptive optics and software to dynamically correct for these variations [77,78]. Spectral excitation selectivity, hence the capacity for multiplexing, can be enhanced by incorporating more than one femtosecond laser in an interline-switched configuration which, as experienced by us and other developers, can satisfactorily separate CFP, GFP, YFP, and RFP, as well as enabling specialized applications, such as sensitized emission-based heterologous FRET [79]. Perhaps the biggest improvements are waiting to be made after the data is collected. High-resolution time-lapse recordings will generate vast amounts of 3D multiplex information. The existing analysis software, however, while allowing breathtaking visualizations, lacks sufficient performance and sophistication for high throughput quantitative analysis of multicellular interactions, requiring involvement of biomathematicians to generate new software tools for such analysis. The cost of Ti-Sapphire lasers and microscope scanners remains high, impeding access to the technology by most laboratories. The development of fiber-based femtosecond lasers, including inexpensive telecommunication-grade ultra short-pulsed lasers, and a strong trend towards simplified, dedicated laser scanners will undoubtedly result in more economical, yet high performance alternatives.

MPM and other high-resolution live tissue imaging techniques heavily depend on various fluorescent dyes and reporters for cell tracking and to assay cell functions. Genetically encoded calcium ion biosensors are one of a great many examples [80]. New fluorescent reporters will be required, whether small molecule chemicals, genetically encoded fluorescent protein, biosensors, or specific promoter-driven constructs, for in vivo visualization of apoptosis, intracellular metabolism, signaling, cytokine production, receptor occupancy, ion channel activity, or electrical potential, for example. To uncover the mechanisms of anti-tumor immune surveillance, researchers will reach for inducible cancer models, which will also help dissecting the role of chronic inflammatory processes and mucosal immune systems in cancer development. New cell lineage-specific fluorescent reporter mice will be instrumental to study stromal cell populations that so far escaped attention, such as MDSC and DC subsets. Protein-linked (as opposed to freely diffusing) fluorescent protein reporter transgenes will be useful to

visualize subcellular distribution and molecular interactions of receptors, signaling proteins, and other proteins in cells in vivo, for example, to reveal immunological synapse formation and cytotoxic granule transfer during CTL killing of cancer cells.

Conclusions

Intravital microscopy, including MPM, is a powerful experimental approach that will foster collaborations between cancer biologist and immunologists and inspire future generations of researchers. It will play increasingly important roles in unraveling the mechanisms of cancer pathogenesis and immune-cancer interactions by characterizing the spatiotemporal regulation of cell–cell, cell–matrix, and molecular interactions under maximally physiological conditions.

Acknowledgments

The study was supported by the National Cancer Institute grant 5R01CA137059 and University of Texas MD Anderson Institutional Research grant 3-0026195. We would like to thank Drs Dimitris Kioussis for the CD2-DsRed mice, Nicholas R.J. Gascoigne for the CD8β-YFP mice, Xiao-Feng Qin for the MCA-mCerulean cells, and Janos Roszik for comments, and our families for their support.

References

1. Peggs KS, Quezada SA, Korman AJ, Allison JP. Principles and use of anti-CTLA4 antibody in human cancer immunotherapy. Curr Opin Immunol 2006;18:206–213. [PubMed: 16464564]
2. Sakaguchi S, Sakaguchi N, Asano M, Itoh M, Toda M. Immunologic self-tolerance maintained by activated T cells expressing IL-2 receptor alpha-chains (CD25). Breakdown of a single mechanism of self-tolerance causes various autoimmune diseases. J Immunol 1995;155:1151–1164. [PubMed: 7636184]
3. Shimizu J, Yamazaki S, Sakaguchi S. Induction of tumor immunity by removing CD25+CD4+ T cells: a common basis between tumor immunity and autoimmunity. J Immunol 1999;163:5211–5218. [PubMed: 10553041]
4. Fontenot JD, Gavin MA, Rudensky AY. Foxp3 programs the development and function of CD4+CD25 + regulatory T cells. Nat Immunol 2003;4:330–336. [PubMed: 12612578]
5. Xu C, Zipfel W, Shear JB, Williams RM, Webb WW. Multiphoton fluorescence excitation: new spectral windows for biological nonlinear microscopy. Science 1996;93:10763–10768.
6. Bush PG, Wokosin DL, Hall AC. Two-versus one photon excitation laser scanning microscopy: critical importance of excitation wavelength. Front Biosci 2007;12:2646–2657. [PubMed: 17127269]
7. Zoumi A, Yeh A, Tromberg BJ. Imaging cells and extracellular matrix in vivo by using second-harmonic generation and two-photon excited fluorescence. Proc Natl Acad Sci USA 2002;99:11014–11019. [PubMed: 12177437]
8. Stoller P, Reiser KM, Celliers PM, Rubenchik AM. Polarization-modulated second harmonic generation in collagen. Biophys J 2002;82:3330–3342. [PubMed: 12023255]
9. Zhuo S, Chen J, Xie S, Hong Z, Jiang X. Extracting diagnostic stromal organization features based on intrinsic two-photon excited fluorescence and second-harmonic generation signals. J Biomed Opt 2009;14:020503. [PubMed: 19405709]
10. Chance B, Schoener B, Oshino R, Itshak F, Nakase Y. Oxidation-reduction ratio studies of mitochondria in freeze-trapped samples. NADH and flavoprotein fluorescence signals. J Biol Chem 1979;254:4764–4771. [PubMed: 220260]
11. Huang S, Heikal AA, Webb WW. Two-photon fluorescence spectroscopy and microscopy of NAD (P)H and flavoprotein. Biophys J 2002;82:2811–2825. [PubMed: 11964266]
12. Nguyen QT, Callamaras N, Hsieh C, Parker I. Construction of a two-photon microscope for video-rate Ca(2+) imaging. Cell Calcium 2001;30:383–393. [PubMed: 11728133]
13. Motoike T, et al. Universal GFP reporter for the study of vascular development. Genesis 2000;28:75–81. [PubMed: 11064424]

14. Amoh Y, Bouvet M, Li L, Tsuji K, Moossa AR, Katsuoka K, Hoffman RM. Visualization of nascent tumor angiogenesis in lung and liver metastasis by differential dual-color fluorescence imaging in nestin-linked-GFP mice. Clin Exp Metastasis 2006;23:315–322. [PubMed: 17136576]
15. Papenfuss HD, Gross JF, Intaglietta M, Treese FA. A transparent access chamber for the rat dorsal skin fold. Microvasc Res 1979;18:311–318. [PubMed: 537508]
16. Falkvoll KH, Rofstad EK, Brustad T, Marton P. A transparent chamber for the dorsal skin fold of athymic mice. Exp Cell Biol 1984;52:260–268. [PubMed: 6734890]
17. Alexander S, Koehl GE, Hirschberg M, Geissler EK, Friedl P. Dynamic imaging of cancer growth and invasion: a modified skin-fold chamber model. Histochem Cell Biol 2008;130:1147–1154. [PubMed: 18987875]
18. Koehl GE, Gaumann A, Geissler EK. Intravital microscopy of tumor angiogenesis and regression in the dorsal skin fold chamber: mechanistic insights and preclinical testing of therapeutic strategies. Clin Exp Metastasis 2009;26:329–344. [PubMed: 19190882]
19. Gligorijevic, B.; Kedrin, D.; Segall, JE.; Condeelis, J.; van Rheenen, J. Dendra2 photoswitching through the Mammary Imaging Window; J Vis Exp. 2009. p. 28http://www.jove.com/index/details.stp?id=1278
20. Sckell A, Klenke FM. The cranial bone window model: studying angiogenesis of primary and secondary bone tumors by intravital microscopy. Methods Mol Biol 2009;467:343–355. [PubMed: 19301683]
21. Lamm WJ, Bernard SL, Wagner WW Jr, Glenny RW. Intravital microscopic observations of 15-microm microspheres lodging in the pulmonary microcirculation. J Appl Physiol 2005;98:2242–2248. [PubMed: 15705726]
22. Myllyharju J, Kivirikko KI. Collagens and collagen-related diseases. Ann Med 2001;33:7–21. [PubMed: 11310942]
23. Provenzano PP, Eliceiri KW, Campbell JM, Inman DR, White JG, Keely PJ. Collagen reorganization at the tumor-stromal interface facilitates local invasion. BMC Med 2006;4:38. [PubMed: 17190588]
24. Skala MC, Squirrell JM, Vrotsos KM, Eickhoff JC, Gendron-Fitzpatrick A, Eliceiri KW, Ramanujam N. Multiphoton microscopy of endogenous fluorescence differentiates normal, precancerous, and cancerous squamous epithelial tissues. Cancer Res 2005;65:1180–1186. [PubMed: 15735001]
25. Vander Heiden, MG.; Cantley, LC.; Thompson, CB. Science. Vol. 324. New York, NY: 2009. Understanding the Warburg effect: the metabolic requirements of cell proliferation; p. 1029-1033.
26. Bartrons R, Caro J. Hypoxia, glucose metabolism and the Warburg's effect. J Bioenerg Biomembr 2007;39:223–229. [PubMed: 17661163]
27. Chen Z, Lu W, Garcia-Prieto C, Huang P. The Warburg effect and its cancer therapeutic implications. J Bioenerg Biomembr 2007;39:267–274. [PubMed: 17551814]
28. Hanahan D, Weinberg RA. The hallmarks of cancer. Cell 2000;100:57–70. [PubMed: 10647931]
29. Skala MC, Riching KM, Gendron-Fitzpatrick A, Eickhoff J, Eliceiri KW, White JG, Ramanujam N. In vivo multiphoton microscopy of NADH and FAD redox states, fluorescence lifetimes, and cellular morphology in precancerous epithelia. Proc Natl Acad Sci USA 2007;104:19494–19499. [PubMed: 18042710]
30. De Giorgi V, Massi D, Sestini S, Cicchi R, Pavone FS, Lotti T. Combined non-linear laser imaging (two-photon excitation fluorescence microscopy, fluorescence lifetime imaging microscopy, multispectral multiphoton microscopy) in cutaneous tumours: first experiences. J Eur Acad Dermatol Venereol 2009;23:314–316. [PubMed: 19207664]
31. Conklin MW, Provenzano PP, Eliceiri KW, Sullivan R, Keely PJ. Fluorescence lifetime imaging of endogenous fluorophores in histopathology sections reveals differences between normal and tumor epithelium in carcinoma in situ of the breast. Cell Biochem Biophys 2009;53:145–157. [PubMed: 19259625]
32. Provenzano PP, Inman DR, Eliceiri KW, Knittel JG, Yan L, Rueden CT, White JG, Keely PJ. Collagen density promotes mammary tumor initiation and progression. BMC Med 2008;6:11. [PubMed: 18442412]
33. Skala MC, Riching KM, Bird DK, Gendron-Fitzpatrick A, Eickhoff J, Eliceiri KW, Keely PJ, Ramanujam N. In vivo multiphoton fluorescence lifetime imaging of protein-bound and free

nicotinamide adenine dinucleotide in normal and precancerous epithelia. J Biomed Opt 2007;12:024014. [PubMed: 17477729]

34. Konig K, Riemann I. High-resolution multiphoton tomography of human skin with subcellular spatial resolution and picosecond time resolution. J Biomed Opt 2003;8:432–439. [PubMed: 12880349]
35. Halin C, Rodrigo Mora J, Sumen C, von Andrian UH. In vivo imaging of lymphocyte trafficking. Annu Rev Cell Dev Biol 2005;21:581–603. [PubMed: 16212508]
36. Cahalan MD, Parker I, Wei SH, Miller MJ. Two-photon tissue imaging: seeing the immune system in a fresh light. Nat Rev Immunol 2002;2:872–880. [PubMed: 12415310]
37. Kedrin D, Wyckoff J, Sahai E, Condeelis J, Segall JE. Imaging tumor cell movement in vivo. Curr Protoc Cell Biol 2007;Chapter 19(Unit 19.7)
38. Sahai E, Wyckoff J, Philippar U, Segall JE, Gertler F, Condeelis J. Simultaneous imaging of GFP. CFP and collagen in tumors in vivo using multiphoton microscopy. BMC Biotechnol 2005;5:14. [PubMed: 15910685]
39. Friedl P, Wolf K. Plasticity of cell migration: a multiscale tuning model. J Cell Biol 2009;188:11–19. [PubMed: 19951899]
40. Friedl P, Wolf K. Tumour-cell invasion and migration: diversity and escape mechanisms. Nat Rev 2003;3:362–374.
41. Wolf K, Mazo I, Leung H, Engelke K, von Andrian UH, Deryugina EI, Strongin AY, Brocker EB, Friedl P. Compensation mechanism in tumor cell migration: mesenchymal-amoeboid transition after blocking of pericellular proteolysis. J Cell Biol 2003;160:267–277. [PubMed: 12527751]
42. Friedl P, Noble PB, Walton PA, Laird DW, Chauvin PJ, Tabah RJ, Black M, Zanker KS. Migration of coordinated cell clusters in mesenchymal and epithelial cancer explants in vitro. Cancer Res 1995;55:4557–4560. [PubMed: 7553628]
43. Hegerfeldt Y, Tusch M, Brocker EB, Friedl P. Collective cell movement in primary melanoma explants: plasticity of cell-cell interaction, beta1-integrin function, and migration strategies. Cancer Res 2002;62:2125–2130. [PubMed: 11929834]
44. Nabeshima K, Moriyama T, Asada Y, Komada N, Inoue T, Kataoka H, Sumiyoshi A, Koono M. Ultrastructural study of TPA-induced cell motility: human well-differentiated rectal adenocarcinoma cells move as coherent sheets via localized modulation of cell-cell adhesion. Clin Exp Metastasis 1995;13:499–508. [PubMed: 7586808]
45. Wolf K, Wu YI, Liu Y, Geiger J, Tam E, Overall C, Stack MS, Friedl P. Multi-step pericellular proteolysis controls the transition from individual to collective cancer cell invasion. Nat Cell Biol 2007;9:893–904. [PubMed: 17618273]
46. Giampieri S, Manning C, Hooper S, Jones L, Hill CS, Sahai E. Localized and reversible TGFbeta signalling switches breast cancer cells from cohesive to single cell motility. Nat Cell Biol 2009;11:1287–1296. [PubMed: 19838175]
47. Quaranta V. Motility cues in the tumor microenvironment. Differentiation 2002;70:590–598. [PubMed: 12492500]
48. Yoo JS, Kim HB, Won N, Bang J, Kim S, Ahn S, Lee BC, Soh KS. Evidence for an additional metastatic route: in vivo imaging of cancer cells in the primo-vascular system around tumors and organs. Mol Imaging Biol. 201010.1007/s11307-010-0366-1
49. Wang W, et al. Single cell behavior in metastatic primary mammary tumors correlated with gene expression patterns revealed by molecular profiling. Cancer Res 2002;62:6278–6288. [PubMed: 12414658]
50. Vishnubhotla R, Sun S, Huq J, Bulic M, Ramesh A, Guzman G, Cho M, Glover SC. ROCK-II mediates colon cancer invasion via regulation of MMP-2 and MMP-13 at the site of invadopodia as revealed by multiphoton imaging. Lab Invest 2007;87:1149–1158. [PubMed: 17876296]
51. Wyckoff JB, Insel L, Khazaie K, Lichtner RB, Condeelis JS, Segall JE. Suppression of ruffling by the EGF receptor in chemotactic cells. Exp Cell Res 1998;242:100–109. [PubMed: 9665807]
52. Wang W, Wyckoff JB, Goswami S, Wang Y, Sidani M, Segall JE, Condeelis JS. Coordinated regulation of pathways for enhanced cell motility and chemotaxis is conserved in rat and mouse mammary tumors. Cancer Res 2007;67:3505–3511. [PubMed: 17440055]

53. Winkler F, Kienast Y, Fuhrmann M, Von Baumgarten L, Burgold S, Mitteregger G, Kretzschmar H, Herms J. Imaging glioma cell invasion in vivo reveals mechanisms of dissemination and peritumoral angiogenesis. Glia 2009;57:1306–1315. [PubMed: 19191326]
54. Kedrin D, Gligorijevic B, Wyckoff J, Verkhusha VV, Condeelis J, Segall JE, van Rheenen J. Intravital imaging of metastatic behavior through a mammary imaging window. Nat Meth 2008;5:1019–1021.
55. Sipkins DA, Wei X, Wu JW, Runnels JM, Cote D, Means TK, Luster AD, Scadden DT, Lin CP. In vivo imaging of specialized bone marrow endothelial microdomains for tumour engraftment. Nature 2005;435:969–973. [PubMed: 15959517]
56. Kienast Y, von Baumgarten L, Fuhrmann M, Klinkert WE, Goldbrunner R, Herms J, Winkler F. Real-time imaging reveals the single steps of brain metastasis formation. Nat Med 2010;16:116–122. [PubMed: 20023634]
57. Xin H, Zhang C, Herrmann A, Du Y, Figlin R, Yu H. Sunitinib inhibition of Stat3 induces renal cell carcinoma tumor cell apoptosis and reduces immunosuppressive cells. Cancer Res 2009;69:2506–2513. [PubMed: 19244102]
58. Murdoch C, Muthana M, Coffelt SB, Lewis CE. The role of myeloid cells in the promotion of tumour angiogenesis. Nat Rev 2008;8:618–631.
59. Wyckoff JB, Wang Y, Lin EY, Li JF, Goswami S, Stanley ER, Segall JE, Pollard JW, Condeelis J. Direct visualization of macrophage-assisted tumor cell intravasation in mammary tumors. Cancer Res 2007;67:2649–2656. [PubMed: 17363585]
60. Leimgruber A, et al. Behavior of endogenous tumor-associated macrophages assessed in vivo using a functionalized nanoparticle. Neoplasia 2009;11:459–468. 452 p following 468. [PubMed: 19412430]
61. Patsialou A, Wyckoff J, Wang Y, Goswami S, Stanley ER, Condeelis JS. Invasion of human breast cancer cells in vivo requires both paracrine and autocrine loops involving the colony-stimulating factor-1 receptor. Cancer Res 2009;69:9498–9506. [PubMed: 19934330]
62. Wyckoff J, Wang W, Lin EY, Wang Y, Pixley F, Stanley ER, Graf T, Pollard JW, Segall J, Condeelis J. A paracrine loop between tumor cells and macrophages is required for tumor cell migration in mammary tumors. Cancer Res 2004;64:7022–7029. [PubMed: 15466195]
63. Fukumura D, Xavier R, Sugiura T, Chen Y, Park EC, Lu N, Selig M, Nielsen G, Taksir T, Jain RK, Seed B. Tumor induction of VEGF promoter activity in stromal cells. Cell 1998;94:715–725. [PubMed: 9753319]
64. Brown EB, Campbell RB, Tsuzuki Y, Xu L, Carmeliet P, Fukumura D, Jain RK. In vivo measurement of gene expression, angiogenesis and physiological function in tumors using multi-photon laser scanning microscopy. Nat Med 2001;7:864–868. [PubMed: 11433354]
65. Perentes JY, McKee TD, Ley CD, Mathiew H, Dawson M, Padera TP, Munn LL, Jain RK, Boucher Y. In vivo imaging of extracellular matrix remodeling by tumor-associated fibroblasts. Nat Methods 2009;6:143–145. [PubMed: 19151720]
66. Dunn GP, Bruce AT, Ikeda H, Old LJ, Schreiber RD. Cancer immunoediting: from immunosurveillance to tumor escape. Nat Immunol 2002;3:991–998. [PubMed: 12407406]
67. Ali S, Ahmad M, Lynam J, Rees RC, Brown N. Trafficking of tumor peptide-specific cytotoxic T lymphocytes into the tumor microcirculation. Int J Cancer 2004;110:239–244. [PubMed: 15069688]
68. Ali SA, Rees RC, Anderson DQ, Reed MW, Goepel JR, Brown NJ. Trafficking of ‘immune’ CD4 (+)/CD8(+)T-lymphocytes into the RENCA tumour microcirculation in vivo in mice. Br J Cancer 2000;83:1061–1068. [PubMed: 10993655]
69. Mrass P, Takano H, Ng LG, Daxini S, Lasaro MO, Iparraguirre A, Cavanagh LL, von Andrian UH, Ertl HC, Haydon PG, Weninger W. Random migration precedes stable target cell interactions of tumor-infiltrating T cells. J Exp Med 2006;203:2749–2761. [PubMed: 17116735]
70. Boissonnas A, Fetler L, Zeelenberg IS, Hugues S, Amigorena S. In vivo imaging of cytotoxic T cell infiltration and elimination of a solid tumor. J Exp Med 2007;204:345–356. [PubMed: 17261634]
71. Breart B, Lemaitre F, Celli S, Bousso P. Two-photon imaging of intratumoral CD8+ T cell cytotoxic activity during adoptive T cell therapy in mice. J Clin Invest 2008;118:1390–1397. [PubMed: 18357341]

72. Mrass P, Kinjyo I, Ng LG, Reiner SL, Pure E, Weninger W. CD44 mediates successful interstitial navigation by killer T cells and enables efficient antitumor immunity. Immunity 2008;29:971–985. [PubMed: 19100702]

73. Mempel TR, Pittet MJ, Khazaie K, Weninger W, Weissleder R, von Boehmer H, von Andrian UH. Regulatory T cells reversibly suppress cytotoxic T cell function independent of effector differentiation. Immunity 2006;25:129–141. [PubMed: 16860762]

74. Boissonnas A, Scholer-Dahirel A, Simon-Blancal V, Pace L, Valet F, Kissenpfennig A, Sparwasser T, Malissen B, Fetler L, Amigorena S. Foxp3+ T cells induce perforin-dependent dendritic cell death in tumor-draining lymph nodes. Immunity 2010;32:266–278. [PubMed: 20137985]

75. McConnell G. Nonlinear optical microscopy at wavelengths exceeding 1.4 microm using a synchronously pumped femtosecond-pulsed optical parametric oscillator. Phys Med Biol 2007;52:717–724. [PubMed: 17228116]

76. Vadakkan TJ, Culver JC, Gao L, Anhut T, Dickinson ME. Peak multiphoton excitation of mCherry using an optical parametric oscillator (OPO). J Fluoresc 2009;19:1103–1109. [PubMed: 19590939]

77. Albert O, Sherman L, Mourou G, Norris TB, Vdovin G. Smart microscope: an adaptive optics learning system for aberration correction in multiphoton confocal microscopy. Opt Lett 2000;25:52–54. [PubMed: 18059779]

78. Marsh P, Burns D, Girkin J. Practical implementation of adaptive optics in multiphoton microscopy. Opt Express 2003;11:1123–1130. [PubMed: 19465977]

79. Zal, MA.; Nelson, M.; Zal, T. Proceedings of SPIE. Vol. 6442. SPIE Publishing; Bellingham: 2007. Interleaved dual-wavelength multiphoton imaging system for heterologous FRET and versatile fluorescent protein excitation.

80. Miyawaki A, Griesbeck O, Heim R, Tsien RY. Dynamic and quantitative Ca2+ measurements using improved cameleons. Proc Natl Acad Sci USA 1999;96:2135–2140. [PubMed: 10051607]

81. Veiga-Fernandes H, Coles MC, Foster KE, Patel A, Williams A, Natarajan D, Barlow A, Pachnis V, Kioussis D. Tyrosine kinase receptor RET is a key regulator of Peyer's Patch organogenesis. Nature 2007;446:547–551. [PubMed: 17322904]

82. Yachi PP, Ampudia J, Gascoigne NRJ, Zal T. Nonstimulatory peptides contribute to antigen-induced CD8-T cell receptor interaction at the immunological synapse. Nat Immunol 2005;6:785–792. [PubMed: 15980863]

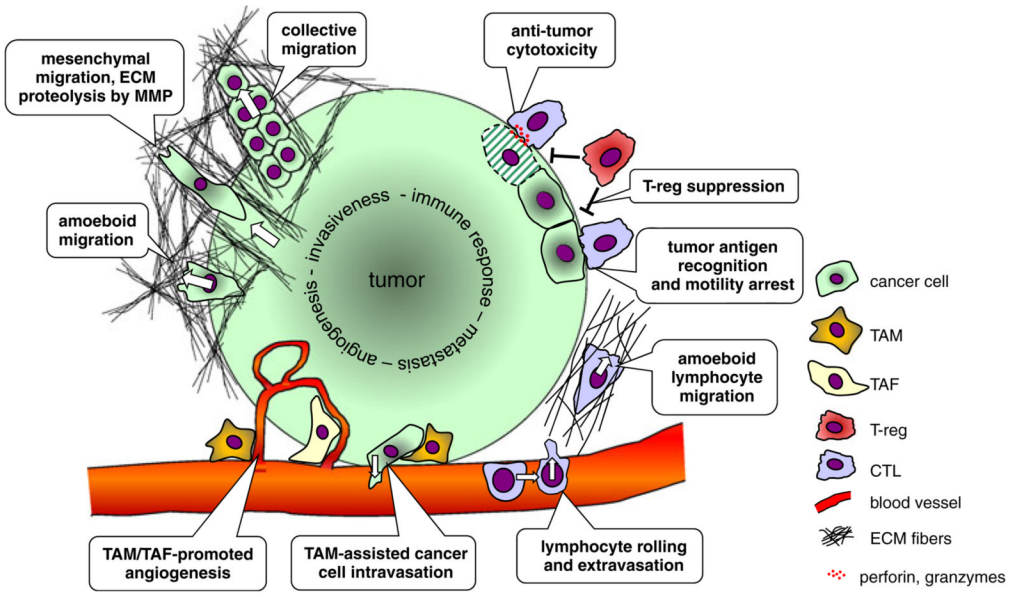

Fig. 1.

Schematic representation of cell–cell and cell–matrix interactions in the tumor microenvironment. At the invasive edge, cancer cells move through the extracellular matrix (ECM) outwards into the surrounding tissue. Two types of translational motility can be distinguished based on cell morphological changes and its interactions with the fibrillar collagen networks. Mesenchymal motility is typical for connective tissue cells and is characterized by matrix metalloproteinase—mediated ECM degradation at the leading cell edge, which leaves tubular tracks that can guide other cells. Collective migration can be regarded as cooperative mesenchymal motility. Amoeboid motility is typical for lymphocytes and occurs without ECM degradation by transient formation of lamellipodia, focal cell attachment, and uropod retraction. Under certain conditions, cancer cell motility can undergo a mesenchymal-amoeboid transition. Tumor-associated macrophages (TAM) and tumor-associated fibroblasts contribute to tumor angiogenesis, and TAM can assist cancer cells intravasating into the lumen of blood vessels. Lymphocyte interactions with tumors involve recruitment from the circulation via integrin-mediated rolling followed by extravasation. Upon amoeboid migration into the tumor mass, tumor antigen-specific cytotoxic T lymphocytes (CTL) can form stable contacts with cancer cells and kill the cells by apoptosis. Regulatory $FoxP3^{+}$ $CD4^{+}$ T cells can interfere with CTL effector function by inhibiting cytotoxic granule release

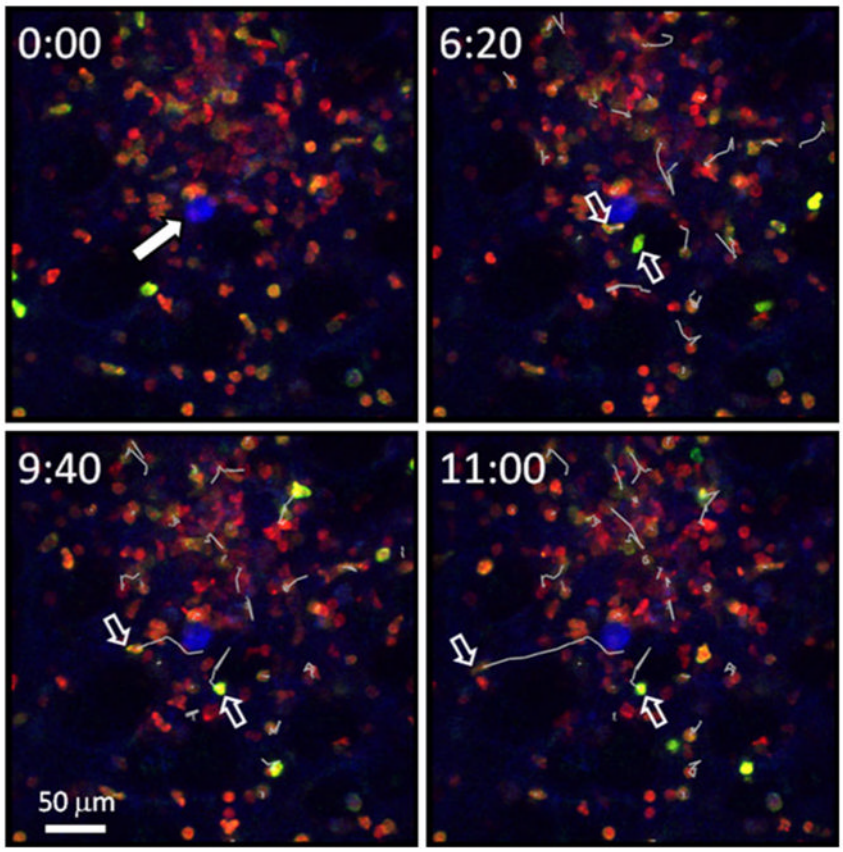

Fig. 2.

Live imaging of T cell recruitment to a lung sarcoma tumor. A dual reporter hCD2p-DsRed × CD8β-YFP mouse was implanted s.c. with the methylcholanthrene (MCA) sarcoma tumor on day 0 to mimic a primary tumor. On day 7, MCA-mCerulean cells were injected i.v. to induce lung metastasis. Intravital microscopy of the lungs was performed on day 8 to visualize cytotoxic T lymphocytes (CTL) recruitment to micrometastases. *Blue*: MCA-mCerulean tumor, *solid arrow; red*: DsRed is expressed in all T cells [81]; *green*: CD8β-YFP chains are expressed on the cell surface only in $CD8^+$ T cells by pairing with CD8*α* chains [82]. Cell tracking analysis was performed on selected $CD8^+$ T cells. Note the two $CD8^+$ T cells (*open arrows*) that extravasate next to the tumor cell at 6 min 20 s and migrate as indicated by the *white tracks*. Data acquisition: Leica SP5RS resonant scanning confocal microscope, ×20 NA 0.95 water immersion objective, 458, 514, and 543 nm excitation. The images represent maximum intensity projections from image stack spaced at *z*=3 μm. Temporal resolution, 20 s. The data provides an example of the benefits of fast resonant scanning confocal microscopy and fluorescent reporter mice for intravital imaging of CTL activity in experimental lung metastases